Absorption profiles of alkali-metal D lines in the presence of a static magnetic field

P. Tremblay, A. Michaud, M. Levesque, S. Thériault, M. Breton, J. Beaubien, and N. Cyr

Centre d'Optique, Photonique et Laser (COPL), Département de Génie Électrique,
Université Laval, Québec (Québec), Canada G1K 7P4

When atoms are placed in a static magnetic field, they undergo shifts of their energy levels and changes in their transition probabilities. These two effects must be taken into account when considering absorption profiles of alkali-metal D lines, which result from the contribution of many transitions influenced by the laser spectrum and Doppler broadening. The model presented here gives the D-lines absorption coefficients of alkali-metal vapors in the presence of an arbitrary static magnetic field. They are evaluated considering various laser polarizations. Experimental measurements of D-line absorption profiles for ^{85}Rb, ^{87}Rb, and ^{133}Cs isotopes show excellent agreement with theoretical predictions.

I. INTRODUCTION

Interaction of laser beams with atoms in the presence of a static magnetic field is encountered in many experiments. Optical pumping of the cesium beam frequency standard under a non-negligible static magnetic field was put forward to increase the pumping efficiency.[1] Variation of the magnetic field has also been proposed to tune semiconductor lasers frequency locked to an alkali-metal D line resonance.[2,3] Finally, cooling experiments on alkali-metal atomic beams use inhomogeneous magnetic fields.[4] The changes in transition probabilities and energy levels caused by the magnetic field must be known in order to evaluate the achievable performances of those experiments.

The absorption profiles of alkali-metal isotopes are particularly sensitive to the perturbation introduced by the presence of the field. One can easily predict the shift and the splitting of the various components of these lines by simply considering the Zeeman structure of the involved energy levels. However, this approach fails to predict the experimentally observed behavior. The lines often continue to be composite and the absorption at each resonance strongly depends on the field value.

We will present the effects of a static magnetic field on both energy levels and transition probabilities by measuring and calculating the D-line linear absorption profiles of alkali-metal atoms placed in such a field. Three different isotopes are used: ^{85}Rb, ^{87}Rb, and ^{133}Cs. We consider the transmission profiles when the interrogating laser is π or σ polarized with respect to the magnetic-field direction.

II. THEORETICAL MODEL

The aim of this section is to calculate the absorption coefficient of an atomic vapor. We first evaluate the effect of the magnetic field on the atomic energies and state vectors and the probabilities of the involved transitions. Only principal polarizations are studied in order to avoid birefringence effects in the absorption cell.

A. Energies and state vectors

The Hamiltonian of the atom in the presence of a static magnetic field **B** is the sum of the unperturbated atomic Hamiltonian $\mathcal{H}_0$ and the Zeeman Hamiltonian,

$$\mathcal{H}_Z = \left(-\frac{\mu_B}{\hbar}\right) \mathbf{B} \cdot (\mathbf{L} + g_S \mathbf{S} + g_I \mathbf{I}). \tag{1}$$

The precise knowledge of the behavior of the atom in such conditions necessitates the evaluation of the energy and the state vector of each particular Zeeman sublevel. Thus we must find the eigenvalues and the eigenvectors of the Hamiltonian.

The direction of the magnetic field defines the quantization axis. We use the basis of the unperturbated atomic state vectors, $|F, m_F\rangle$. Under this representation, the diagonal matrix elements of the Hamiltonian become

$$\langle F, m_F | \mathcal{H} | F, m_F \rangle = E_0(F) - \mu_B g_F m_F B_z, \tag{2}$$

where $E_0(F)$ is the energy of the sublevel $|F, m_F\rangle$ and g_F is the associated Landé factor. The off-diagonal matrix elements may be nonzero only between $\Delta F = \pm 1$, $\Delta m_F = 0$ sublevels,

$$\langle F - 1, m_F | \mathcal{H} | F, m_F \rangle = \langle F, m_{F_a} | \mathcal{H} | F - 1, m_F \rangle$$

$$= -\frac{\mu_B}{2}(g_J - g_I)B_z \left(\frac{[(J + I + 1)^2 - F^2][F^2 - (J - I)^2]}{F}\right)^{1/2} \left(\frac{F^2 - m_F^2}{F(2F + 1)(2F - 1)}\right)^{1/2}. \tag{3}$$
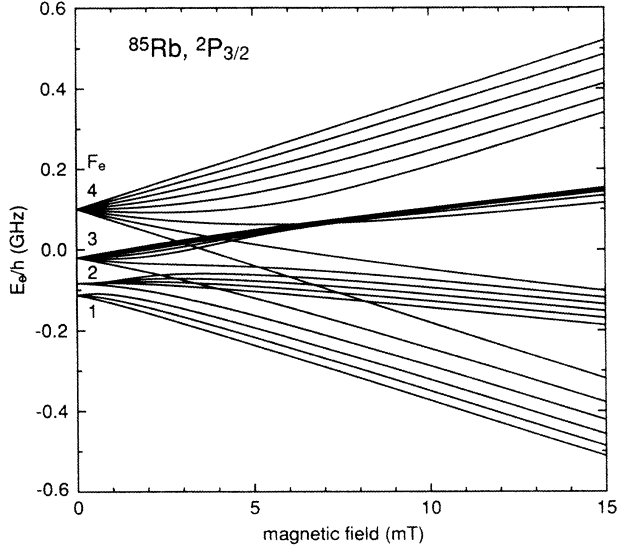
FIG. 1.   Zeeman structure of the $^2P_{3/2}$ state of ^{85}Rb.

The matrix representing the Hamiltonian is then block diagonal, each block corresponding to a given m_F.

Our goal being the evaluation of absorption profiles, we have to consider atomic transitions between the sublevels of the ground state and those of an excited state. Thus, the evaluation of the new energies and state vectors must be done for both states. The eigenvalues give the energy levels E_e or E_g, and the new state vectors can be expressed in terms of the unperturbated atomic state vectors,

$$|\psi(F_e, m_e)\rangle = \sum_{F_e'} c_{F_e F_e'} |F_e', m_e\rangle \qquad (4)$$

and

$$|\psi(F_g, m_g)\rangle = \sum_{F_g'} c_{F_g F_g'} |F_g', m_g\rangle , \qquad (5)$$

where the sums are done only on state vectors having the same m_F since the perturbation introduced by the magnetic field couples only sublevels with $\Delta m_F = 0$.

As an example, the Zeeman structure of the $^2P_{3/2}$ excited state of ^{85}Rb is given in Fig. 1. This behavior compares with that obtained for ^{133}Cs by Hirano.[5] Even at 1 mT the low-field approximation is no longer valid.

B. Transition probabilities

The laser light influence on the atom is taken into account by an interaction term coupling the atomic electric dipole and the oscillating laser electric field, $-\mathbf{D} \cdot \mathbf{E}(t)$. The time-dependent perturbation approach gives the well-known result for the transition probability,

$$W_{eg} = \frac{|\langle e| \mathbf{D} \cdot \mathbf{e} |g\rangle|^2 E^2}{4\hbar^2} \delta(\nu - \nu_{eg} - \mathbf{v} \cdot \mathbf{k}/2\pi), \qquad (6)$$

where E and $\mathbf{e}$ are, respectively, the electric-field amplitude and unit vector, ν is the laser frequency, ν_{eg} is the transition frequency $[(E_e - E_g)/h]$, $\mathbf{v}$ is the atomic velocity, and $\mathbf{k}$ is the propagation vector. The electric dipole moment is expressed in terms of standard components,

$$\mathbf{D} \cdot \mathbf{e} = \sum_q D_q e_q, \qquad (7)$$

where $q = -1, 0, 1$.

Each matrix element of a given electric dipole component D_q is proportional to the spontaneous emission rate of the associated transition A_{eg},[6]

$$|\langle e| D_q |g\rangle|^2 = \frac{3\epsilon_0 \hbar \lambda_{eg}^3}{8\pi^2} A_{eg}. \qquad (8)$$

The spontaneous emission rates are proportional to the square of the transfer coefficients modified by the presence of the magnetic field,

$$A_{eg} = \Gamma_e \, a^2[\psi(F_e, m_e); \psi(F_g, m_g); q]. \qquad (9)$$

These "modified" transfer coefficients are expressed as

$$a[\psi(F_e, m_e); \psi(F_g, m_g); q]$$

$$= \sum_{F_e', F_g'} c_{F_e F_e'} \, a(F_e', m_e; F_g', m_g; q) \, c_{F_g F_g'}, \qquad (10)$$

where $a(F_e, m_e; F_g, m_g; q)$ are the unperturbated transfer coefficients having the following definition:[6]

$$a(F_e, m_e; F_g, m_g; q) = (-1)^{1+I+J_e+F_e+F_g-m_e} \sqrt{2J_e+1}\sqrt{2F_e+1}\sqrt{2F_g+1} \begin{pmatrix} F_e & 1 & F_g \\ -m_e & q & m_g \end{pmatrix} \begin{Bmatrix} F_e & 1 & F_g \\ J_g & I & J_e \end{Bmatrix}, \qquad (11)$$

the parentheses and curly brackets denote, respectively, the 3-j and 6-j coefficients.[7]

The finite lifetime of the excited state causes the transition frequencies to spread into a Lorentzian profile of full width at half maximum $\Delta\nu_e$. Moreover, we consider a laser having a Lorentzian spectral profile of full width at half maximum $\Delta\nu$, which is the expected behavior for semiconductor lasers.[8] The transition probability must then be averaged over these two densities. The Dirac δ function appearing in Eq. (6) then becomes

$L_{\Delta\nu_e+\Delta\nu}(\nu - \nu_{eg} - \mathbf{v} \cdot \mathbf{k}/2\pi)$, where $L_{\Delta\nu}(\nu)$ is the normalized Lorentzian profile centered about zero.

Given the previous considerations, the transition probability between sublevels $|\psi(F_e, m_e)\rangle$ and $|\psi(F_g, m_g)\rangle$ is finally expressed as

$$W_{eg} = \sum_q \frac{3\lambda_{eg}^3}{8\pi hc} A_{eg} e_q^2 I L_{\Delta\nu_e+\Delta\nu}(\nu - \nu_{eg} - \mathbf{v} \cdot \mathbf{k}/2\pi), \qquad (12)$$
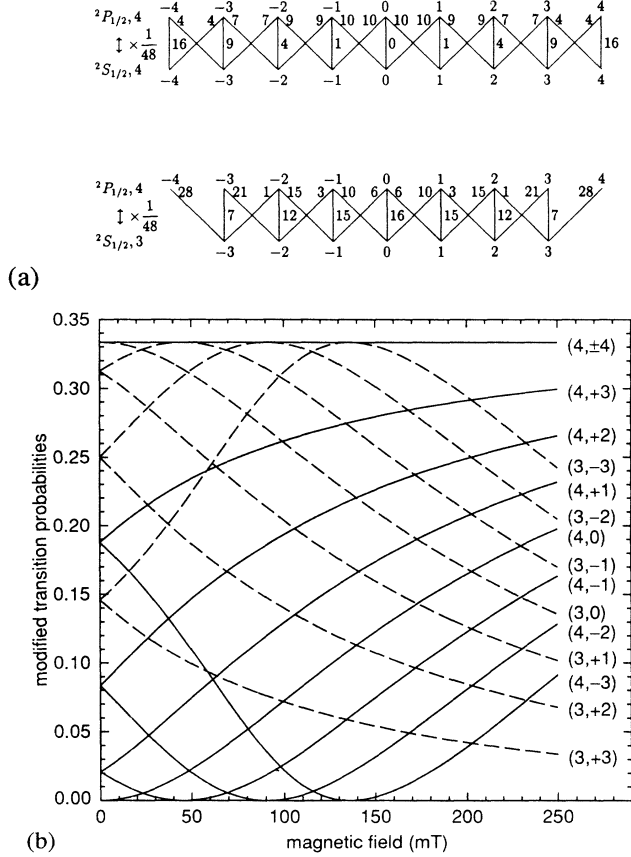
(a)

(b)

FIG. 2. (a) Zero-field transition probabilities and (b) modified transition probabilities, $a^2[\psi(F_e, m_e); \psi(F_g, m_g); q]$, for the $^2S_{1/2}$, $F_g = 3, 4$ to $^2P_{1/2}$, $F_e = 4$ transitions (D_1 line) in π polarization of ^{133}Cs as a function of the magnetic-field intensity.

where I is the laser intensity,

$$I = \tfrac{1}{2}\epsilon_0 c E^2. \tag{13}$$

In order to illustrate the effect of the magnetic field on the transition probabilities, we present the modified transfer coefficients for the $^2S_{1/2}$ to $^2P_{1/2}$ transition of ^{133}Cs (Fig. 2). The usual transfer coefficients are given in Fig. 2(a). They correspond to the starting points ($B_z = 0$) of the curves shown in Fig. 2(b). As one can see, the transition probabilities are greatly modified under the presence of a magnetic field; some transitions vanish for specific field intensities, and $\Delta F = 0$, $\Delta m_F = 0$, or $\Delta F = \pm 2$ transitions are even possible.

C. Absorption coefficient

The absorption coefficient of an atomic vapor is related to the difference between absorption and stimulated emission rates for each particular transition, normalized by the laser intensity in photons per second,

$$\alpha = \sum_{e,g} \frac{W_{eg}}{I/h\nu}(n_g - n_e). \tag{14}$$

The sum is done over all possible transitions, the excited- and ground-state sublevels $|\psi(F_e, m_e)\rangle$ and $|\psi(F_g, m_g)\rangle$ being simply denoted e and g, respectively.

We restrict the study to weak laser intensities. The populations of the various sublevels are then simply given by the Boltzman distribution, thus being independent of laser intensity.

The absorption coefficient becomes

$$\alpha = \sum_{e,g} \sum_q \frac{3\lambda_{eg}^2}{8\pi} A_{eg} e_q^2(n_g - n_e)$$
$$\times L_{\Delta\nu_e + \Delta\nu}(\nu - \nu_{eg} - \mathbf{v} \cdot \mathbf{k}/2\pi). \tag{15}$$

The vapor containing atoms with random velocities, the absorption coefficient must be averaged over all possible velocities, using a Maxwell distribution. This results in a Voigt profile which corresponds to the convolution between Lorentzian and Gaussian profiles,

$$V_{\Delta\nu_e + \Delta\nu, \Delta\nu_D}(\nu) = L_{\Delta\nu_e + \Delta\nu}(\nu) \circ G_{\Delta\nu_D}(\nu), \tag{16}$$

where $\Delta\nu_D$ is the Doppler linewidth.

The absorption coefficient of the vapor averaged over the atomic velocities finally becomes

$$\alpha = \sum_{e,g} \sum_q \frac{3\lambda_{eg}^2 \Gamma_e}{8\pi} a^2[\psi(F_e, m_e); \psi(F_g, m_g); q] e_q^2$$
$$\times (n_g - n_e) V_{\Delta\nu_e + \Delta\nu, \Delta\nu_D}(\nu - \nu_{eg}). \tag{17}$$

The absorption profile is obtained by evaluating the optical transmission of the vapor using this last absorption coefficient,

$$T(\nu) = e^{-\alpha\ell}, \tag{18}$$

where ℓ is the length of the absorption cell.

The different physical parameters used through the calculations were taken from the following references: Nesmeyanov[9] for atom densities, National Bureau of Standards tables[10] for nominal wavelengths, Heavens[11] for excited-state lifetimes, and Arimondo[12] for hyperfine splittings. The laser linewidth was estimated from data obtained in beat experiments. It was found to be around 20 MHz. The length of the absorption cells was 1 cm for ^{85}Rb, and 1.7 cm for the other isotopes. The temperature of the cell was about 25°C.

III. RESULTS

We measured the D_1 and D_2 lines absorption profiles of three different alkali-metal isotopes (^{85}Rb, ^{87}Rb, and ^{133}Cs) in the presence of magnetic fields smaller than 250 mT. All these experiments were done using laser light propagating in a direction perpendicular to the magnetic field ($\mathbf{k} \perp \mathbf{B}$). The light polarization was linear, and parallel or perpendicular to the field axis, thus exciting, respectively, π (e $\|$ **B**: $e_0 = 1$ and $e_{\pm 1} = 0$) or σ transitions (e $\perp$ **B**: $e_0 = 0$ and $|e_{\pm 1}| = 1/\sqrt{2}$).
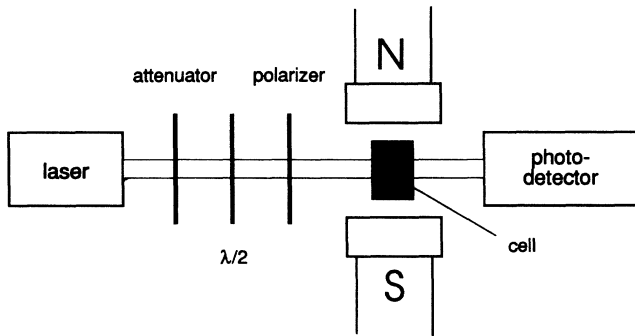
FIG. 3. Experimental setup used to measure the absorption profiles of alkali-metal vapors in the presence of a static magnetic field.
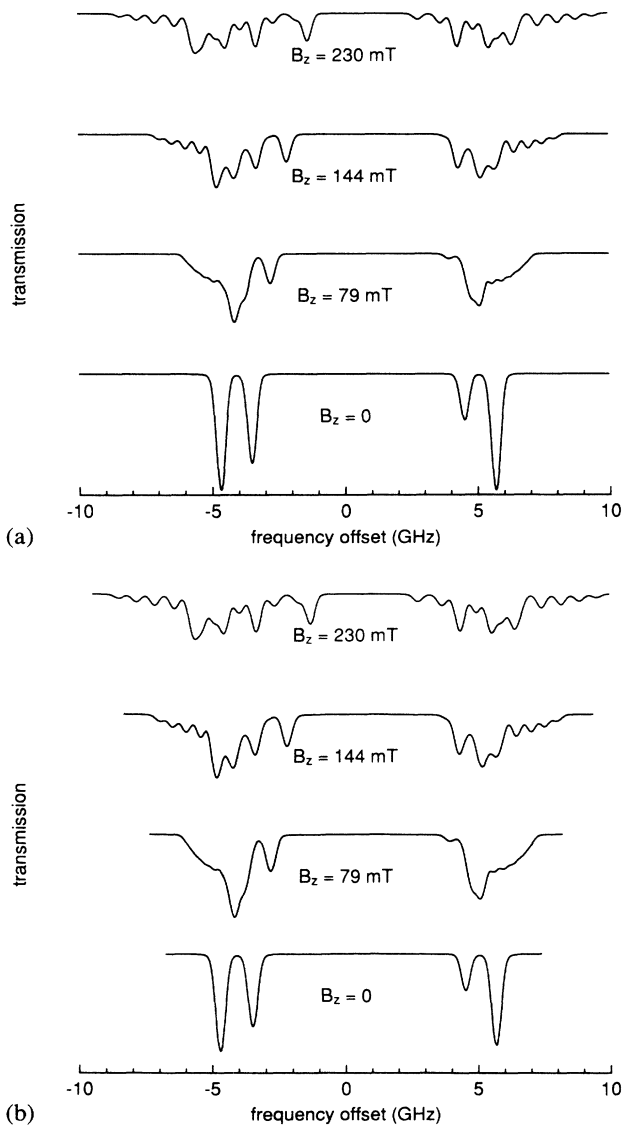
A. Experimental setup

The absorption profiles were measured by sweeping the frequency of a single-mode semiconductor laser. The experimental setup used is depicted in Fig. 3. An attenuator was used to keep the intensity of the light beam entering the atomic cell below 10 μW/cm^2. This level prevented optical pumping effects such as saturation and frequency shifts. The light polarization was adjusted with respect to the magnetic-field direction using a halfwave plate and a polarizer.

The atomic cell was put in a region of the homogeneous static magnetic field created by an electromagnet. The magnet had flat poles with a diameter of 6 cm separated by a distance of 3.6 cm. The laser beam waist was 2 × 8 mm^2. The magnetic-field strength was measured with a commercial Hall effect gaussmeter. A numerical calculation based on finite-element analysis predicted magnetic-field variations of less than 1% over the entire laser-atom interaction region inside the cell. The field could thus be considered constant along the path of the laser in the absorption cell. The predicted magnetic field uniformity was experimentally verified over the region of interest.

B. Absorption profiles

The measured profiles have been normalized to eliminate the variation of laser output power occurring when its injection current is swept. The frequency axis was calibrated by comparing measured and calculated profiles at zero magnetic field. From that, the nonlinearity has been evaluated to be less than 1% of the considered range. Hence the frequency sweep was assumed to be linear.

Figure 4 presents typical results showing the modifica-

FIG. 4. (a) Theoretical and (b) experimental absorption profiles of the ^{133}Cs D_1 line for π transitions and increasing magnetic field. The ordinate scale factors are the same for all curves.
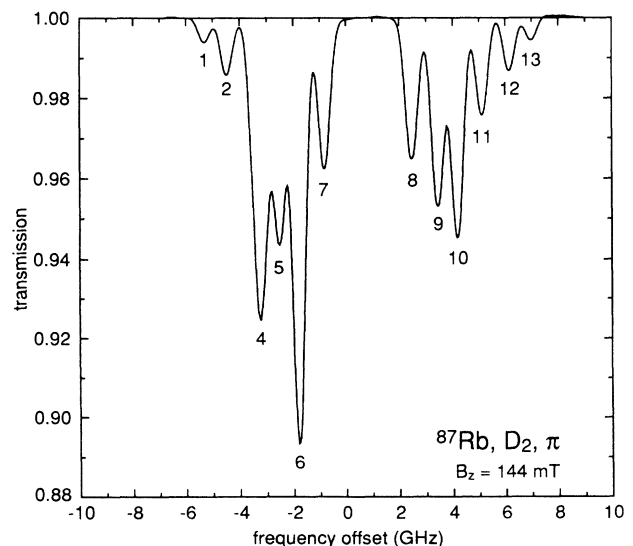

FIG. 5. Typical absorption profile showing identification of the resonances.

tions arising when the field intensity is increased. The components measured at zero field partially divide into many components whose frequency and depth change as the field intensity is varied. The various measured absorption lines correspond to those predicted. This agreement would not have been possible without considering the modifications of the transition probabilities.

C. Resonance frequencies

A total of 100 sweeps have been performed for the various lines of the three isotopes, for π and σ laser polar-

izations, and for ten different field intensities. In order to extract more information from the large amount of data collected, we evaluated the frequencies and depths of the resonances appearing in the various absorption profiles. Figure 5 shows a typical profile. For all of them, we identified the different transmission minima, noting their frequencies and depths. Those values have been plotted against the magnetic field and compared to theoretical predictions.

The results obtained for the resonance frequencies were compiled for both types of excitation of the D_1 and D_2 lines of [85]Rb and [87]Rb isotopes (Figs. 6 and 7), and for the D_1 line of [133]Cs isotope (Fig. 8). Theoretical pre-
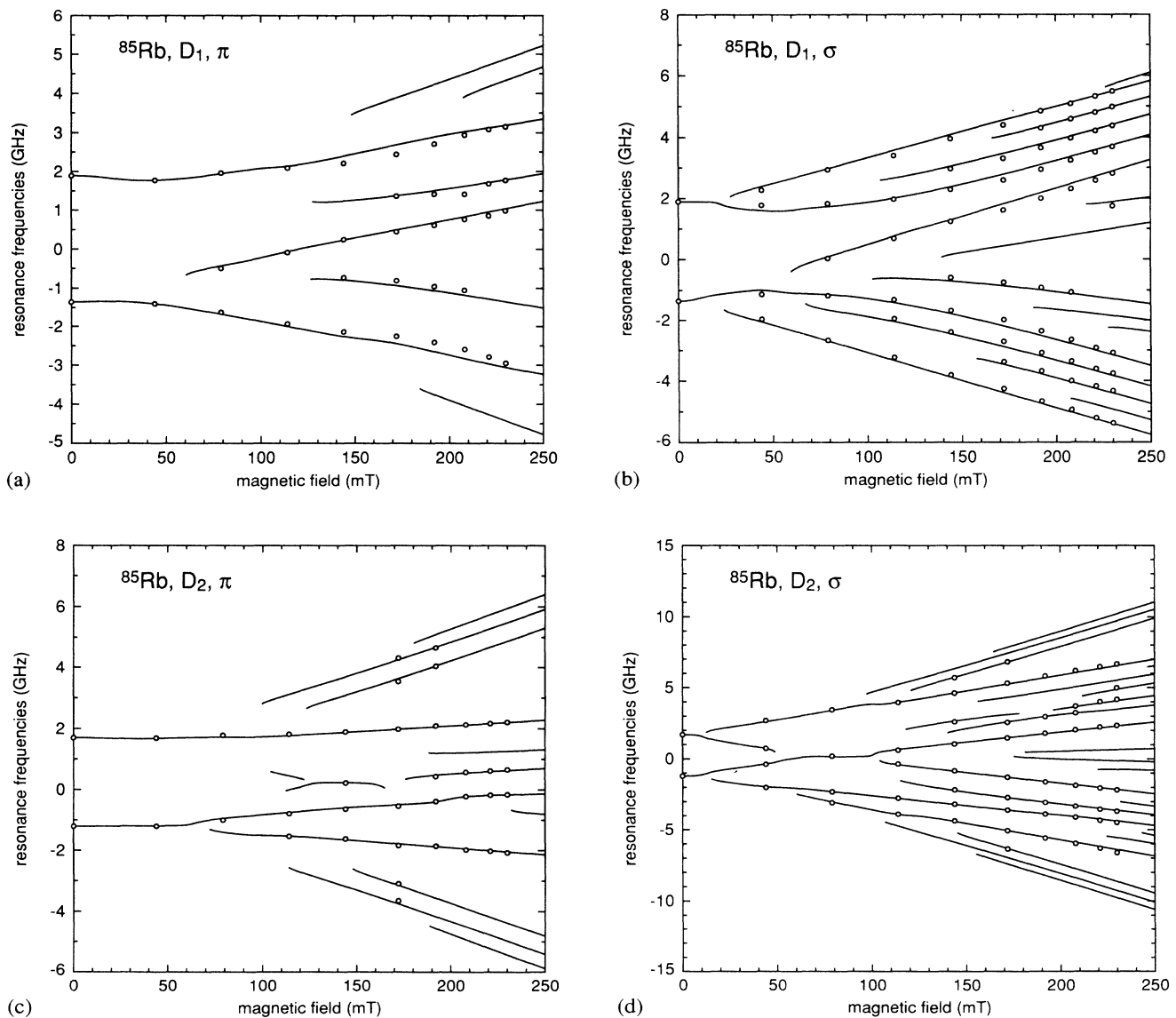

FIG. 6. Experimental (o) and theoretical (—) resonance frequencies of the absorption profiles of the [85]Rb as a function of the field intensity. The curves are given for (a) π and (b) σ polarizations for the D_1 line, and for (c) π and (d) σ polarizations for the D_2 line.
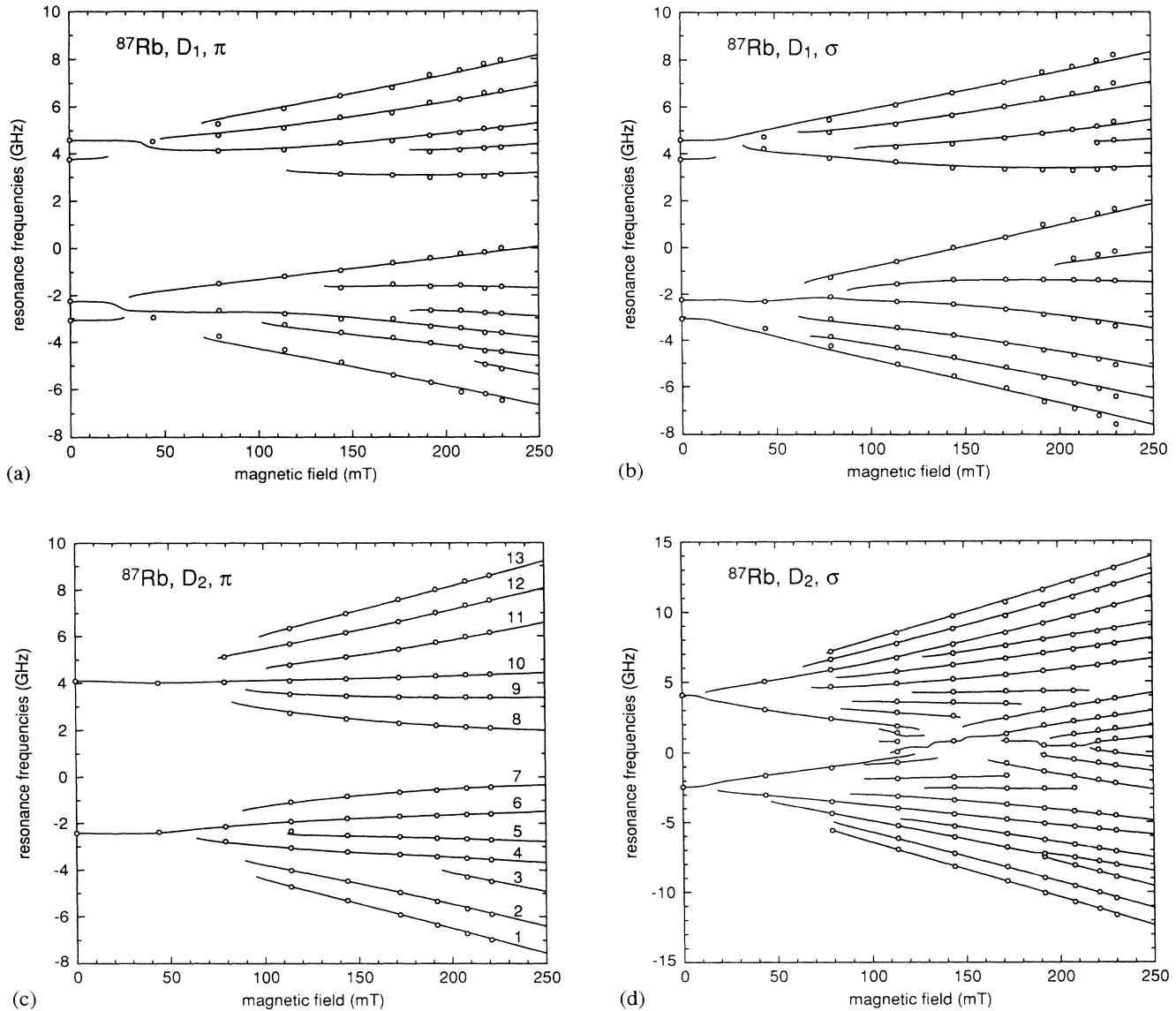
FIG. 7. Experimental (o) and theoretical (—) resonance frequencies of the absorption profiles of the ^{87}Rb as a function of the field intensity. The curves are given for (a) π and (b) σ polarizations for the D_1 line, and for (c) π and (d) σ polarizations for the D_2 line.

dictions appear as solid lines, while circles represent experimental results. Despite small discrepancies that can be explained mainly by imprecisions in the measurement of the absolute field intensity (± 5 mT), the agreement is very good.

Each of those figures (Figs. 6–8) exhibits interesting features in regions where resonances appear or disappear. When two resonances approach each other, they overlap and a mutual pulling of their minima occurs. These will continue to get closer until the minimum of the weaker resonance suddenly disappears. After that, the two resonances are no longer resolved. This phenomenon appears

in Figs. 6–8 as sudden changes in the slope of the curves. Figure 7(d) is particularly interesting in that sense, since many resonances cross each other.

Furthermore, changes in the relative transition probabilities as well as crossings of the transition frequencies contribute to the disappearance of some resonances when the field is varied. For example, in Fig. 8(a), there is a resonance vanishing for 110 mT $\leq B_z \leq$ 160 mT. A look at Fig. 2(b) shows that the transition $F_g = 4$, $m_g = -3 \leftrightarrow F_e = 4$, $m_e = -3$ has a very weak probability for B_z around 135 mT. For that reason, this resonance is not sufficiently important to be observed in the vicinity
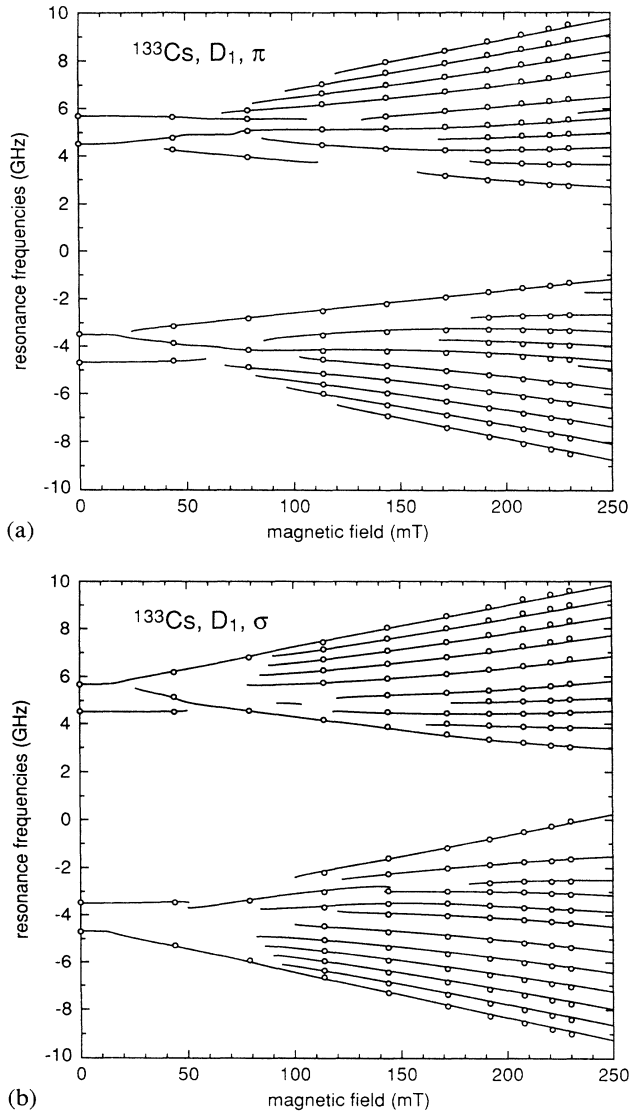
FIG. 8. Experimental (o) and theoretical (—) resonance frequencies of the absorption profiles of the ^{133}Cs as a function of the field intensity. The curves are given for (a) π and (b) σ polarizations for the D_1 line.

FIG. 9. Experimental (o) and theoretical (—) resonances depths of the absorption profiles of the ^{87}Rb as a function of the field intensity. The curves are given for π polarization for the D_2 line.

of that field value.

Finally, Fig. 9 depicts a typical graph obtained when we plot the depth of the resonances against the magnetic field. It compares quite well to the theoretical predictions, the differences being mainly related to the evaluation of the atom density through empirical laws.
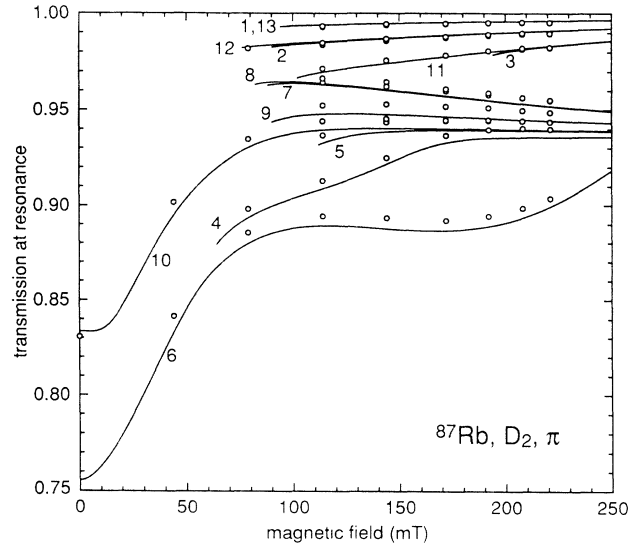
IV. CONCLUSION

The absorption profiles of various alkali-metal isotopes have been measured and calculated under various static magnetic fields. They agree very well in showing that important changes in atomic energy levels and transition probabilities arise even at low-magnetic-field intensities for the ^2P states of alkali-metal atoms. Among the most interesting results obtained through this study are the vanishing of some transitions for specific field intensities, and the appearance of $\Delta F = 0$, $\Delta m_F = 0$, or $\Delta F = \pm 2$ transitions, which are forbidden for $B_z = 0$.

ACKNOWLEDGMENTS

[1]G. Théobald *et al.*, in *Frequency Standards and Metrology, Proceedings of the Fourth Symposium*, edited by A. de Marchi (Springer-Verlag, Berlin, 1989), pp. 110–115.
[2]M. Têtu *et al.*, J. Lightwave Technol. **LT-7**, 1540 (1989).
[3]T. Ikegami, S.-I. Ohshima, and M. Ohtsu, Jpn. J. Appl.

Phys. Lett. **28**, L1839 (1989).
[4]J. Prolan *et al.*, Phys. Rev. Lett. **54**, 992 (1985).
[5]I. Hirano, Metrologia **21**, 27 (1985).
[6]É. de Clercq *et al.*, J. Phys. (Paris) **45**, 239 (1984).
[7]A. Messiah, *Mécanique Quantique* (Dunod, Paris, 1959),

Vol. 2.

[8] K. Vahala and A. Yariv, IEEE J. Quantum Electron. **QE-19**, 1102 (1983).

[9] A.N. Nesmeyanov, *Vapour Pressure of the Elements* (Academic, New York, 1963).

[10] J. Reader, C.H. Corliss, W.L. Wiese, and G.A. Martin, *Wavelengths and Transition Probabilities for Atoms and Atomic Ions* (U.S. GPO, Washington, D.C., 1980).

[11] O.S. Heavens, J. Opt. Soc. Am. **51**, 1058 (1961).

[12] E. Arimondo, M. Inguscio, and P. Violino, Rev. Mod. Phys. **49**, 31 (1977).